

Title: Far-from-equilibrium dynamics of a strongly coupled non-Abelian plasma with non-zero charge density or external magnetic field

Date: Oct 08, 2015 01:00 PM

URL: <http://pirsa.org/15100033>

Abstract: <p>Using holography, we study the evolution of a spatially homogeneous, far from equilibrium, strongly coupled $N=4$ supersymmetric Yang-Mills plasma with a non-zero charge density or a background magnetic field. This gauge theory problem corresponds, in the dual gravity description, to an initial value problem in Einstein-Maxwell theory with homogeneous but anisotropic initial conditions. We explore the dependence of the equilibration process on different aspects of the initial departure from equilibrium and, while controlling for these dependencies, examine how the equilibration dynamics are affected by the presence of a non-vanishing charge density or an external magnetic field. The equilibration dynamics are remarkably insensitive to the addition of even large chemical potentials or magnetic fields, the equilibration time is set primarily by the form of the initial departure from equilibrium. For initial deviations from equilibrium which are well localized in scale, we formulate a simple model for equilibration times which agrees quite well with our results.</p>

John P. Fuhr II

Far from equilibrium
dynamics of a strongly coupled
non-abelian plasma with non-zero
charge density in external
magnetic field

with Ludmilla Yaffe

JHEP02(2015)148

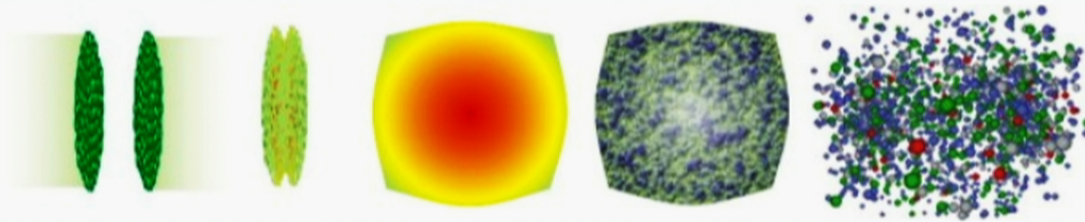


Outline

- Motivation
- Proxy Field Theory
 - $N=4$ SYM + EM
- Holographic Implementation
 - Solving Maxwell-Einstein
- Results
 - Neutral Plasma
 - Charged Plasma
 - Magnetized Plasma
- Discussion
 - Simple Model

Motivation

- Want to understand **strongly coupled** and **far-from-equilibrium** QCD plasma.

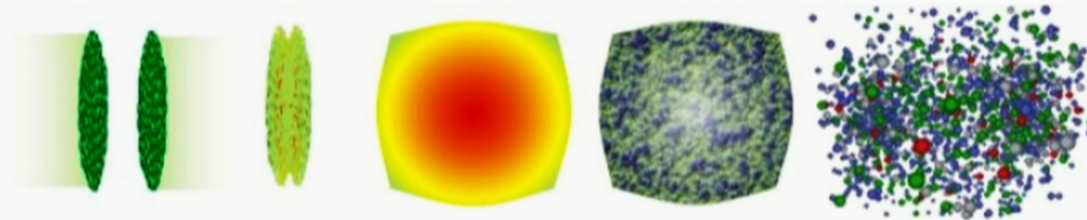


- Gauge/gravity duality (Holography) examines certain **strongly coupled** gauge theories by considering gravity.
- Numerical techniques allow us to study **far-from-equilibrium** dynamics.

The problem of a strongly coupled, far-from-equilibrium plasma turns into a calculation of numerical General Relativity.

Motivation

- Heavy Ion Collisions have a small but finite chemical potential and associated baryon density (**charge density**)
- Large but transient **EM fields** may play a significant role in Heavy Ion Collisions, despite small coupling



Our Field Theory

Simplest Gauge/Gravity example is $\mathcal{N} = 4$ SYM $SU(N_c)$
qualitatively good **toy theory** for QCD

- on 4d minkowski space
- translational inv., x-y rotation inv.
- **couple conserved current** of $U(1)$ subgroup of $SU(4)_R$ global symmetry to a **background Abelian gauge field**.

Trace Anomaly

$$A_{\alpha}^{\text{ext}}(x) \equiv \mu \delta_{\alpha}^0 + \frac{1}{2} \mathcal{B} (x^1 \delta_{\alpha}^2 - x^2 \delta_{\alpha}^1)$$

- chemical potential μ (conjugate to **charge density** in equilibrium) adds a scale, but does not effect the tracelessness of $T^{\alpha\beta}$
- In contrast, the **magnetic field** effects the microscopic dynamics - generates a **non-zero trace anomaly**:

$$T^{\alpha}_{\alpha} = -\frac{1}{4} \kappa (F_{\mu\nu}^{\text{ext}})^2 = -\frac{1}{2} \kappa \mathcal{B}^2$$

$$\kappa \equiv (N_c^2 - 1)/(2\pi^2)$$

- implies **logarithmic dependence** on renormalization point

Proxy Field Theory

Enlarged Theory

$$A_{\alpha}^{\text{ext}}(x) \equiv \frac{1}{2} \mathcal{B} (x^1 \delta_{\alpha}^2 - x^2 \delta_{\alpha}^1)$$

For the magnetic case, it is convenient to interpret the trace anomaly by considering the enlarged theory:

$\mathcal{N} = 4$ SYM $SU(N_c)$ + EM, with total Action

$$S_{\text{SYM+EM}} = S_{\text{SYM, min. coupled}} + S_{\text{EM}}$$

$$S_{\text{EM}} \equiv - \int d^4x \frac{1}{4e^2} F_{\mu\nu}^2$$

- where the electromagnetic coupling e is arbitrarily weak \rightarrow EM fields are classical background fields
- SYM fields charged under this $U(1)$ cause a running coupling (four fermions and three complex scalars)

Scale Dependence

$$\mu \frac{d}{d\mu} e^{-2} \equiv \beta_{1/e^2}(e^{-2}) = -b_0 + O(e^2)$$



$$b_0 \equiv \kappa \left[\frac{1}{6} \sum_{\alpha} (q_f^{\alpha})^2 + \frac{1}{12} \sum_a (q_s^a)^2 \right]$$

Just like charge renormalization in weakly coupled QED

How much of the stress energy comes from the background gauge field?

Total stress energy well-defined, **partitioning is ambiguous**

$$T_{\text{tot}}^{\alpha\beta} \equiv T_{\text{EM}}^{\alpha\beta}(\mu) + \Delta T_{\text{SYM}}^{\alpha\beta}(\mu) \quad T_{\text{EM}}^{\alpha\beta}(\mu) \equiv \frac{1}{e^2(\mu)} \left[F^{\alpha\nu} F^{\beta}_{\nu} - \frac{1}{4} \eta^{\alpha\beta} F^{\mu\nu} F_{\mu\nu} \right]$$

Just like charge renormalization in weakly coupled QED

How much of the stress energy comes from the background gauge field?

Total stress energy well-defined, **partitioning is ambiguous**

$$T_{\text{tot}}^{\alpha\beta} \equiv T_{\text{EM}}^{\alpha\beta}(\mu) + \Delta T_{\text{SYM}}^{\alpha\beta}(\mu) \quad T_{\text{EM}}^{\alpha\beta}(\mu) \equiv \frac{1}{e^2(\mu)} [F^{\alpha\nu} F^{\beta}_{\nu} - \frac{1}{4}\eta^{\alpha\beta} F^{\mu\nu} F_{\mu\nu}]$$

scale dependence between each piece must cancel...

$$\mu \frac{d}{d\mu} \Delta T_{\text{SYM}}^{\alpha\beta}(\mu) = -\mu \frac{d}{d\mu} T_{\text{EM}}^{\alpha\beta}(\mu) = b_0 [F^{\alpha\nu} F^{\beta}_{\nu} - \frac{1}{4}\eta^{\alpha\beta} F^{\mu\nu} F_{\mu\nu}]$$

$\varepsilon(\mu) \equiv \Delta T_{\text{SYM}}^{00}(\mu)/\kappa$ specialized to zero-temperature, ground state energy density:

$$\varepsilon(\mu) = c_0 \mathcal{B}^2 - \frac{1}{4} \mathcal{B}^2 \ln(|\mathcal{B}|/\mu^2)$$

$$\varepsilon_L \equiv \varepsilon(1/L), \quad \varepsilon_{\mathcal{B}} \equiv \varepsilon(|\mathcal{B}|^{1/2})$$

Isotropization/Equilibration

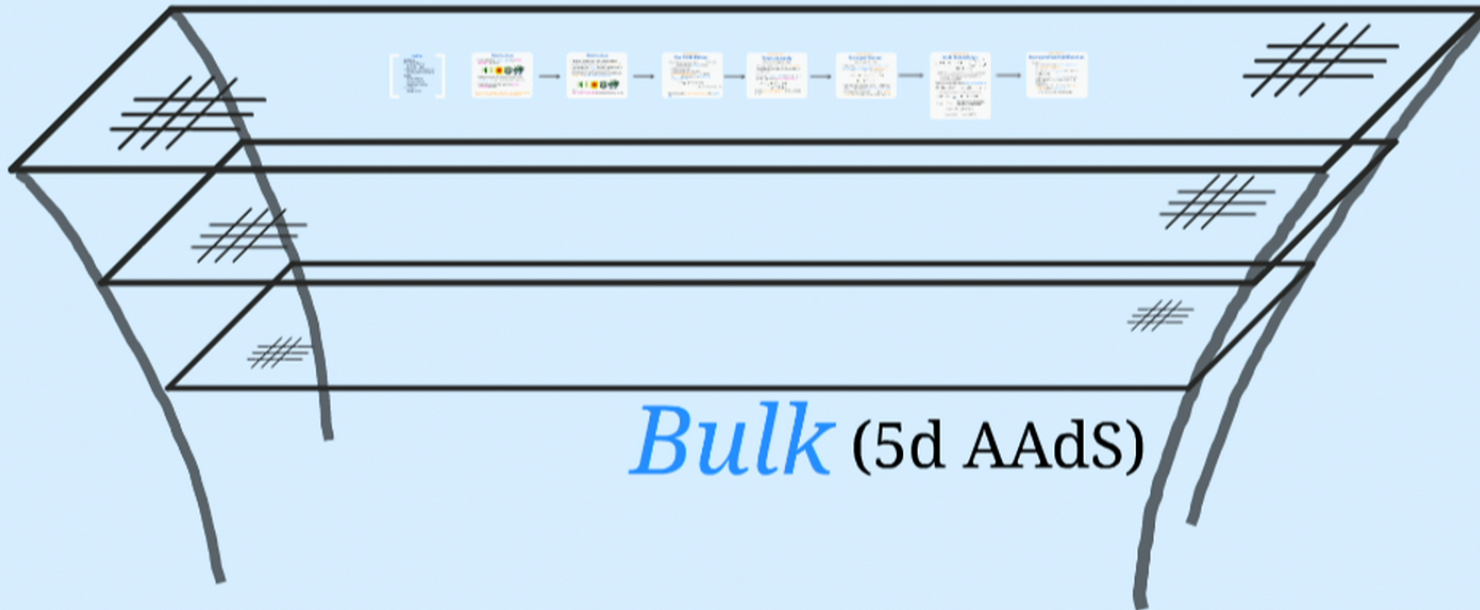
We want:

- to set initial state in some **far-from-equilibrium** and **anisotropic configuration**
- to watch the **stress-energy tensor** evolve in time as the system settles

Boundary (4d Minkowski)

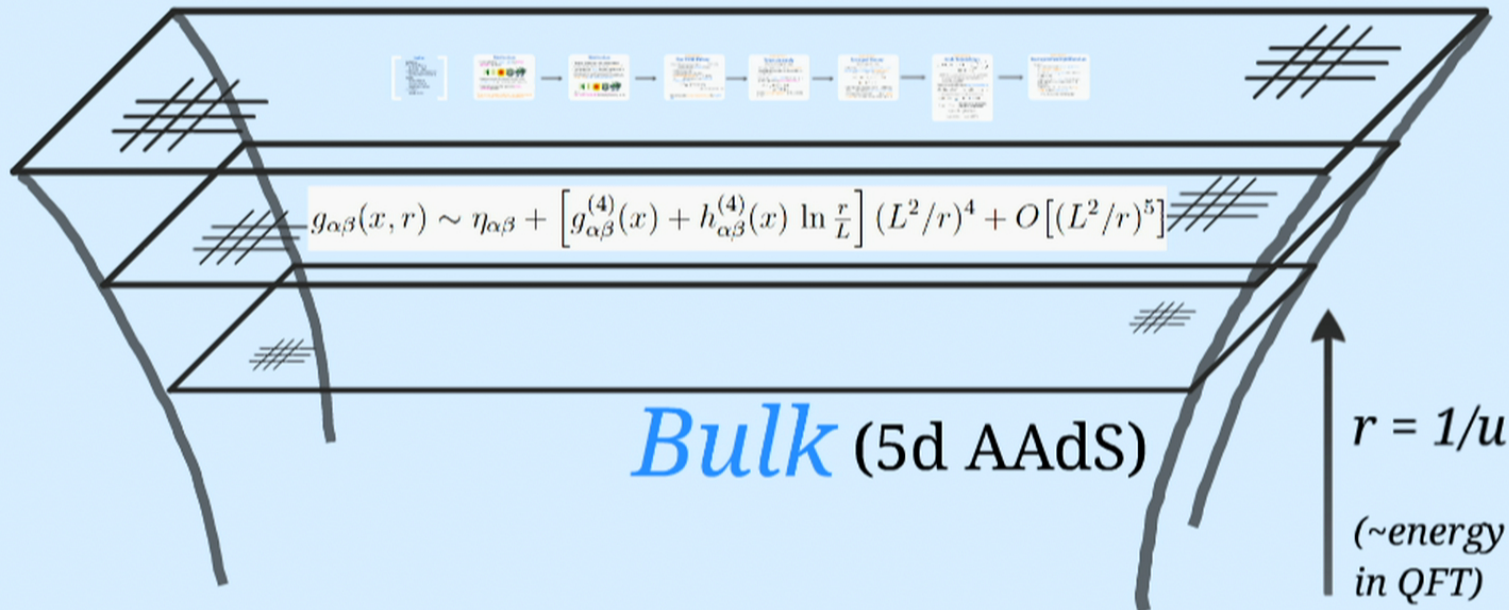


Boundary (4d Minkowski)

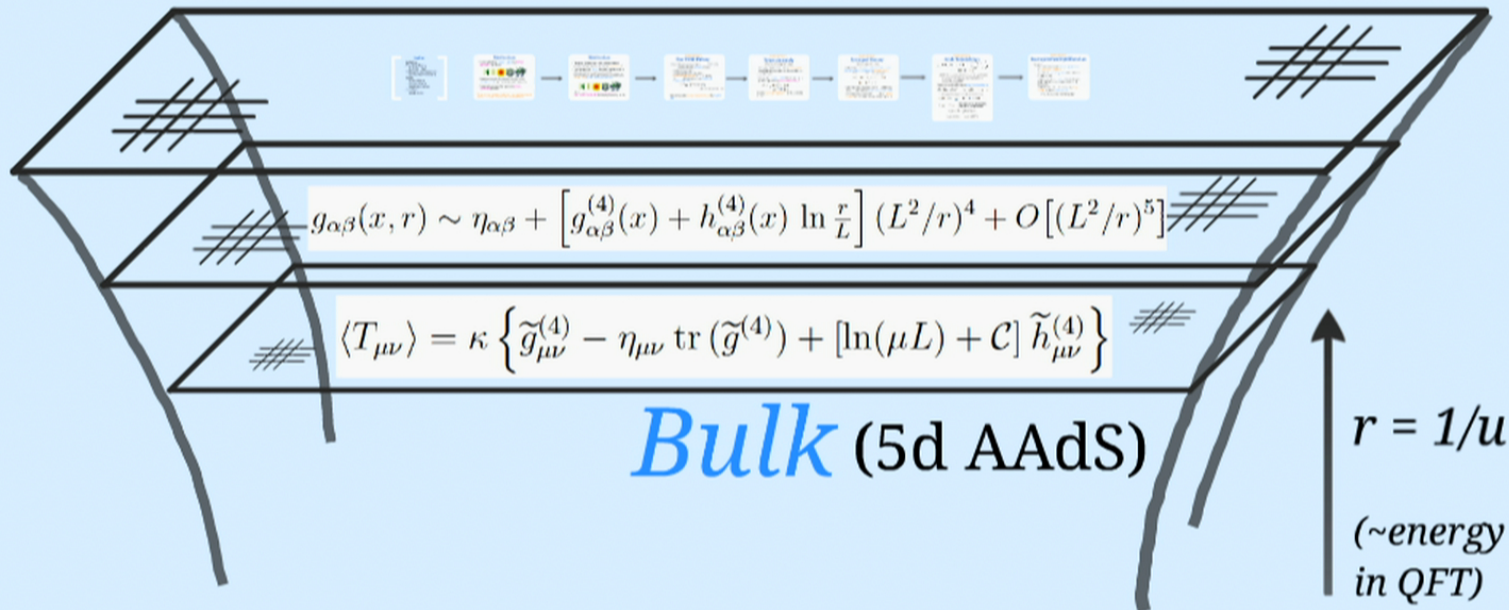


Bulk (5d AAdS)

Boundary (4d Minkowski)



Boundary (4d Minkowski)



Holographic Implementation

Bulk Action

Consistent truncation (top-down construction) for our boundary theory, $S = S_{\text{SYM}} + \int d^4x j^\alpha(x) A_\alpha^{\text{ext}}(x)$ gives **Einstein + Maxwell**:

$$S_5 \equiv \frac{1}{16\pi G_5} \int d^5x \sqrt{-G} (R - 2\Lambda - L^2 F_{MN} F^{MN})$$

$$G_5 \equiv \frac{\pi}{2} L^3 / N_c^2 \quad \Lambda \equiv -6/L^2$$

- 5d Chern-Simons term could be present, but not relevant if only turning on **charge density** OR **magnetic field**

Methods: Setup

Coordinate Choice

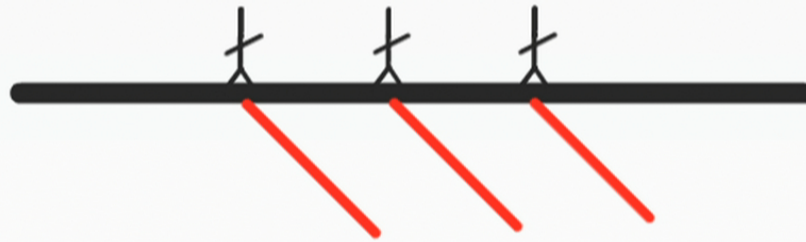
Following *Chesler, Yaffe arXiv:1309.1439*, we chose generalized Eddington Finklestein coordinates:

$$\{ \underline{v, x, y, z}, r \}$$

Boundary coordinates

$$ds^2 = \frac{r^2}{L^2} g_{\mu\nu}(x, r) dx^\mu dx^\nu - 2\omega_\mu(x) dx^\mu dr$$

- coordinates remain regular across future horizon
- infalling radial null geodesics (affine parameter, r)



Ansatz/Symmetries

Since we are interested in homogenous isotropization, we demand the following:

- trans. invariance in x, y, z
- rot. invariance in x - y plane

Bulk Metric

$$ds^2 = -A(v, r)dv^2 + 2drdv + \Sigma(v, r)^2 \left(e^{\underline{B(v,r)}}(dx^2 + dy^2) + e^{-2\underline{B(v,r)}}dz^2 \right)$$

- anisotropy isolated in B
- at the boundary, v coincides with boundary time t .
- radial diffeomorphism freedom $r \rightarrow r + \lambda(v)$

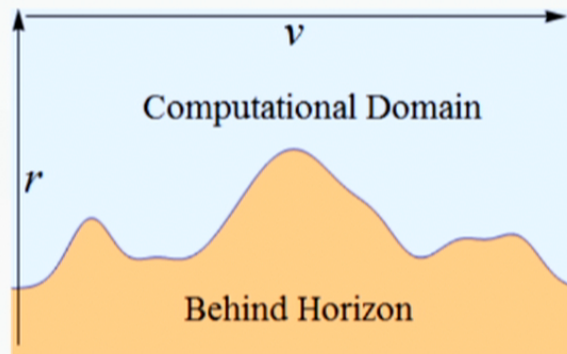
Methods: Solving Radially

Horizon Fixing

Our residual radial gauge, $\lambda(v)$, must be chosen.

$$r \rightarrow r + \lambda(v)$$

We use this freedom to "fix" the horizon.



Holographic Implementation

Field Equations

Maxwell's EQs give: $F_{xy}(x, r) \equiv \mathcal{B} = \text{const}$

$$F_{rv}(x, r) \equiv \mathcal{E}(v, r) = \rho L \Sigma^{-3}(v, r)$$

Einstein EQs give: $\rightarrow \Sigma'' + \frac{1}{2}(B')^2 \Sigma = 0,$

$$A'' - 6(\Sigma'/\Sigma^2) d_+ \Sigma + \frac{3}{2} B' d_+ B = +\frac{5}{3} \mathcal{B}^2 L^2 e^{-2B} \Sigma^{-4} + \frac{7}{3} \mathcal{E}^2 L^2 - 2/L^2$$

$$(d_+ B)' + \frac{3}{2}(\Sigma'/\Sigma) d_+ B + \frac{3}{2} B' (d_+ \Sigma)/\Sigma = -\frac{2}{3} \mathcal{B}^2 L^2 e^{-2B} \Sigma^{-4},$$

$$(d_+ \Sigma)' / \Sigma + 2(\Sigma'/\Sigma^2) d_+ \Sigma = -\frac{1}{3} \mathcal{B}^2 L^2 e^{-2B} \Sigma^{-4} - \frac{1}{3} \mathcal{E}^2 L^2 + 2/L^2$$

$$d_+(d_+ \Sigma) - A' (d_+ \Sigma) + \frac{1}{2} \Sigma (d_+ B)^2 = 0,$$

$$d_+ \equiv \partial_v + A(v, r) \partial_r$$

At some initial time, v_0 , Given: $\varepsilon, \lambda, B(v_0, r)$ and $(\rho$ or $\mathcal{B})$

System reduces to nested set of **radial ODEs**

Methods: Solving Asymptotically

Asymptotic Solutions

Expand each function in a truncated expansion, e.g.

$$u = \sum_{n=0}^{\infty} \sum_{m=0}^{\infty} c_{nm} \epsilon^n v^m$$

- solve order by order to find $u_0(\epsilon)$
- up to two unknown coefficients in each function - using with nested gauge parameter $\delta(\epsilon)$
- enforce matching boundary the leading order

$$\lim_{\epsilon \rightarrow 0} \frac{1}{\delta(\epsilon)} u(\delta, \epsilon) = u_0 \quad (0 < \delta \ll \epsilon)$$

- matching terms must be found from asymptotic theory - the coefficient terms give the unknown gauge terms



Methods: Solving Radially

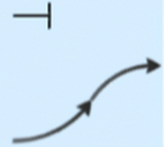
Radial Solver Choice

~~Finite Difference Methods~~

- subdivide intervals - e.g. distributions appear, using for grid refinement
- error - for radial ρ method gaussian (GMC) scheme, ρ is the number of points
- difficulty handling singularity in EOMs

~~Spectral Methods~~

- spectral grid, or collocation points, optimized
- derivatives approx. using full domain - global
- error - exponential decrease in number of points
- very easy to handle singularity in EOMs



Methods: Solving Radially

Spectral Methods

$$\mathcal{L}f(x) = q_0(x)f''(x) + q_1(x)f'(x) + q_2(x)f(x) = S(x)$$

$$f(x) = \sum_{n=0}^{\infty} c_n P_n(x) \quad \mathcal{L}P_n(x) = \lambda_n P_n(x)$$

Interpolated solutions on a periodic domain, a Chebyshev grid appears:

$$f(x) = \sum_{n=0}^N c_n T_n(x) \quad T_n(x) = \cos(n \arccos(x))$$

- values at collocation points equal to series of Chebyshev functions

$$f(x) = \sum_{n=0}^N c_n T_n(x) \quad \mathcal{L}f(x) = S(x)$$

- Derivatives become matrices
- $\mathcal{L}T_n = \lambda_n T_n$, $\mathcal{L}T_0 = \mathcal{L}T_1 = \mathcal{L}T_2 = 0$
- coefficients of Chebyshev simply evaluating $f(x)$ at $x_j = \cos(\frac{j\pi}{N})$, $\mathcal{L}f(x) = S(x)$



Methods: Solving Radially

Spectral Methods (cont)

Tricky parts are:

- how to choose collocation points?
- which Chebyshev functions to use?
- how to handle divergence in differential equation?

For a finite, non-periodic domain, best choice is a Gauss-Lobatto grid, and Chebyshev Polys.

As for the divergence:

- remove off asymptotic pieces of function
- spectral method receives a row and replaces with boundary condition - remove divergent row, replace with boundary condition the substituted function

Holographic Implementation

Time Stepping

Once we have d_+B and B' on a given timeslice v_0 ,
(as well as our other metric functions)

$$\partial_v B(v_0, r) = d_+B(v_0, r) - A(v_0, r) \partial_r B(v_0, r)$$

The stationarity condition on the horizon gives us $\partial_v \lambda$

Integrate forward, $v_0 \rightarrow v_0 + \Delta v$, with a Runge-Kutta 4th
order method to find:

$$B(v_0 + \Delta v), \quad \lambda(v_0 + \Delta v)$$

- Restart the entire radial process, now on the new timeslice
- **watch system equilibrate**

Results

Equilibrium Configurations

Neutral Plasma

$$(\rho = 0, \mathcal{B} = 0)$$

Equilibrates to Schwarzschild Black Brane:

$$ds^2 = -U(\tilde{r}) dt^2 + \frac{d\tilde{r}^2}{U(\tilde{r})} + \frac{\tilde{r}^2}{L^2} (dx^i)^2$$

$$U(\tilde{r}) \equiv \frac{\tilde{r}^2}{L^2} - \frac{m L^2}{\tilde{r}^2}$$

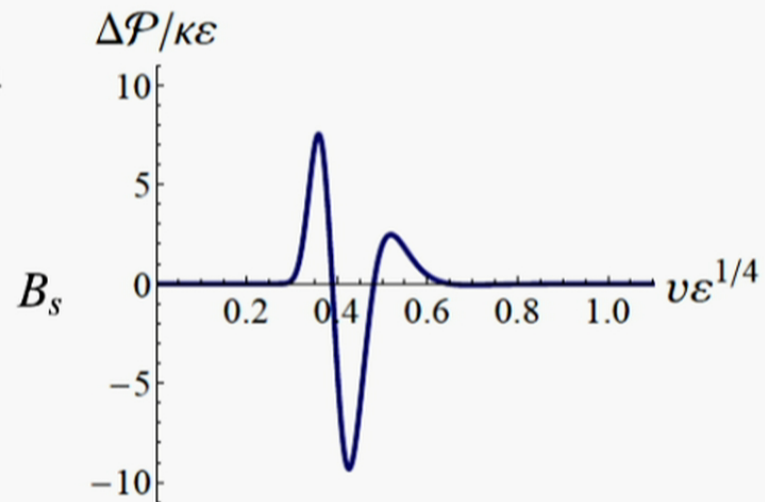
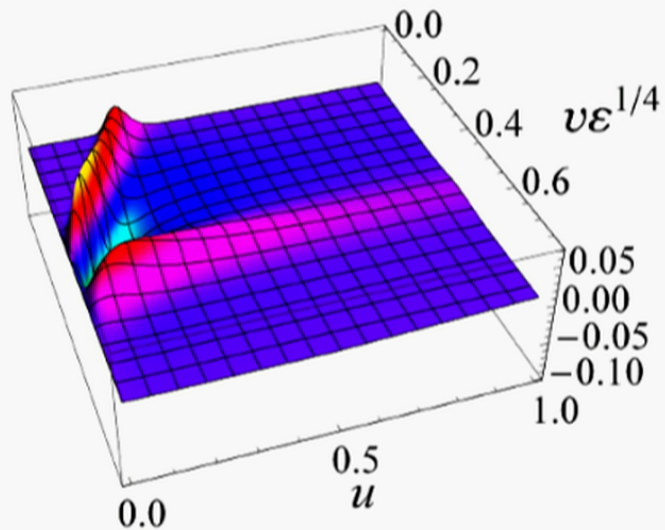
$$\varepsilon = \frac{3}{4} m L^{-4} = \frac{3}{4} (\pi T)^4$$

Results: Neutral Plasma

General Evolution

$$B(v_0, r) = \mathcal{A} e^{-\frac{1}{2}(r-r_0)^2/\sigma^2}$$

$$\Delta \mathcal{P} \equiv \frac{1}{2}(T^{11} + T^{22}) - T^{33}$$



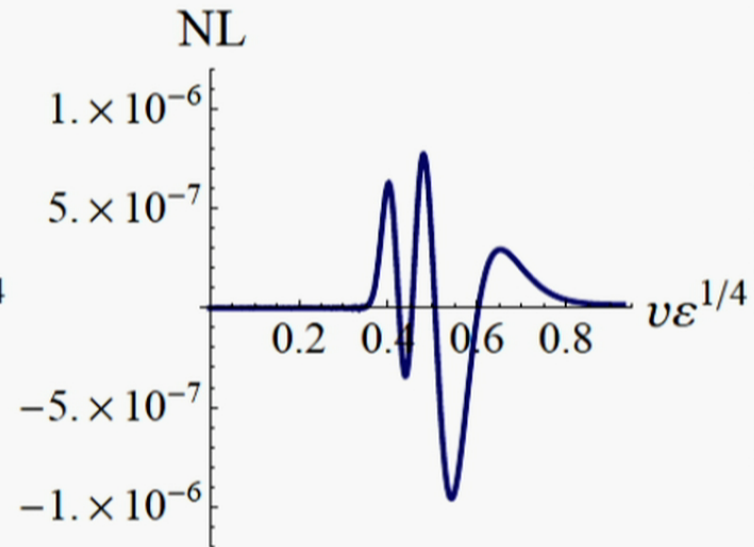
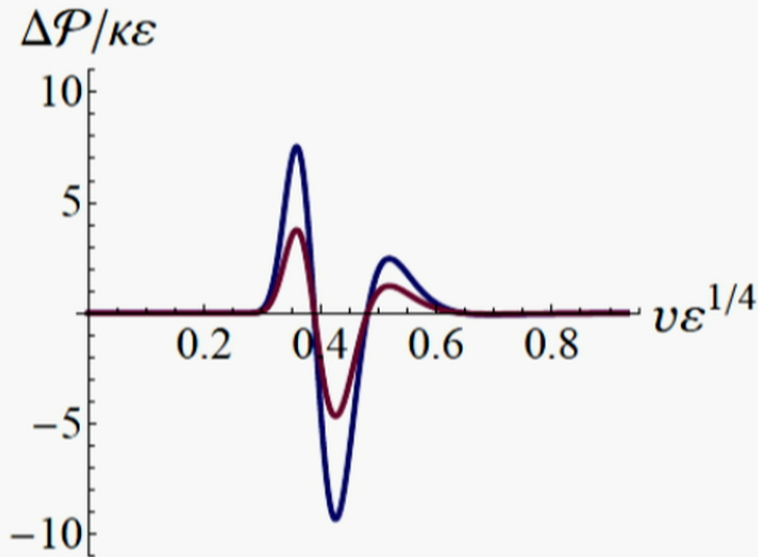
Results: Neutral Plasma

Sensitivity to Gaussian

$$B(v_0, r) = \mathcal{A} e^{-\frac{1}{2}(r-r_0)^2/\sigma^2}$$

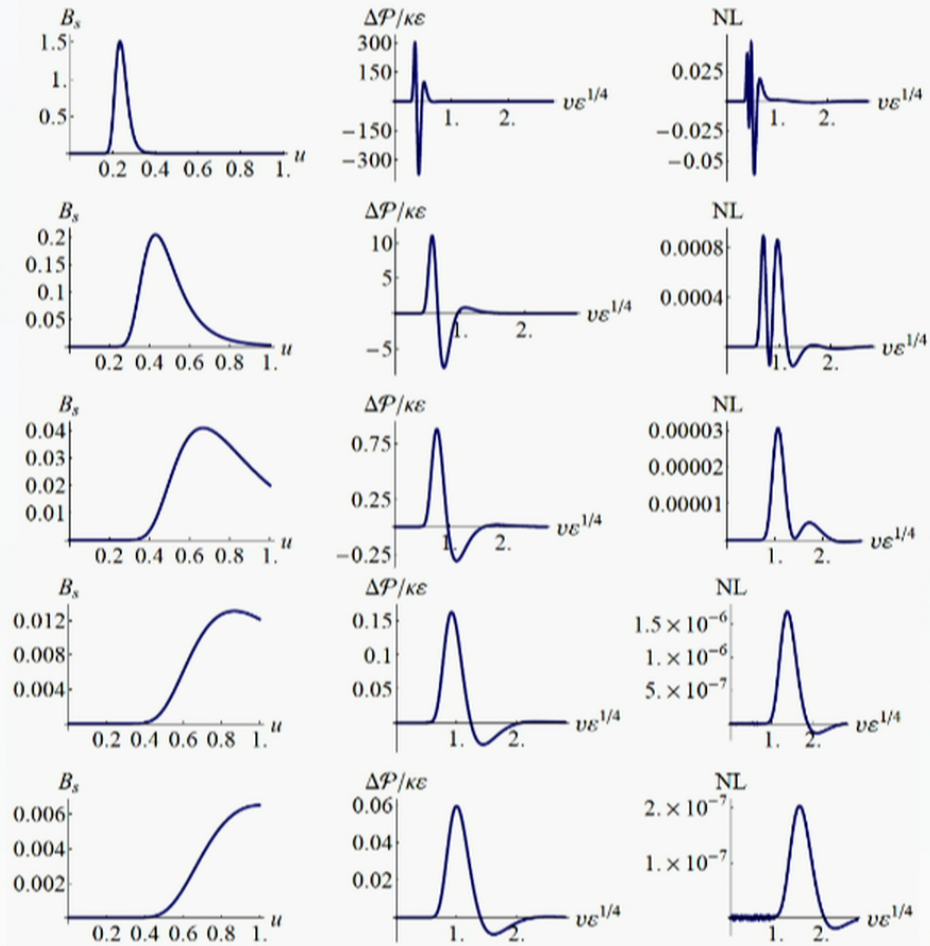
- Amplitude and r_0 interesting

Amplitude test. Double initial Gaussian's Amp, check results.



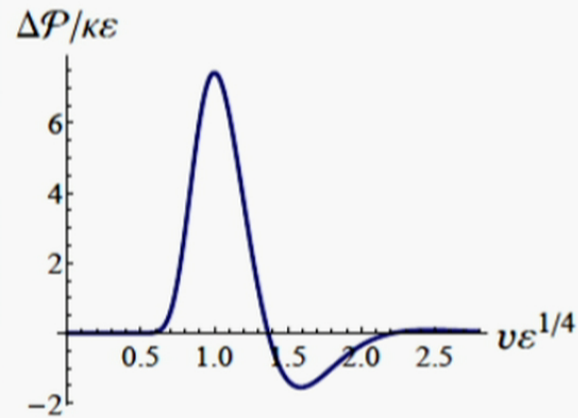
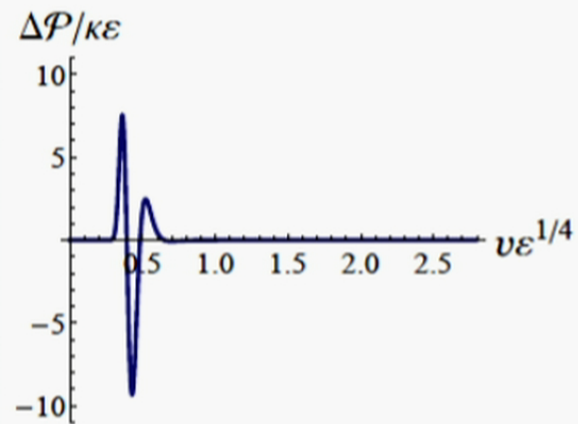
Results: Neutral Plasma

Depth & Non-linearities



Results: Neutral Plasma

Matched Bndry Anisotropy



Charged Plasma

$$(\rho \neq 0, \mathcal{B} = 0)$$

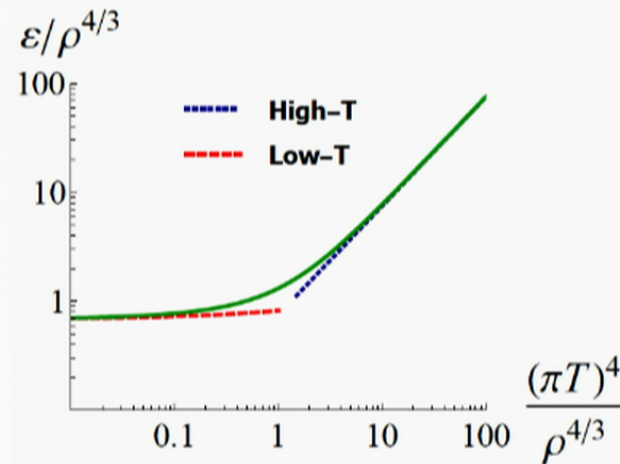
Equilibrates to Reissner-Nordstrom Black Brane

Myers et al. hep-th/9902170

$$ds^2 = -U(\tilde{r}) dt^2 + \frac{d\tilde{r}^2}{U(\tilde{r})} + \frac{\tilde{r}^2}{L^2} (dx^i)^2$$

$$U(\tilde{r}) \equiv \frac{\tilde{r}^2}{L^2} - m \frac{L^2}{\tilde{r}^2} + \frac{1}{3} (\rho L^3)^2 \frac{L^4}{\tilde{r}^4}$$

$$(\rho_{\max} L^3)^4 = \frac{4}{3} m^3 \quad \mu = \frac{1}{2} \rho (L^2 / \tilde{r}_h)^2$$

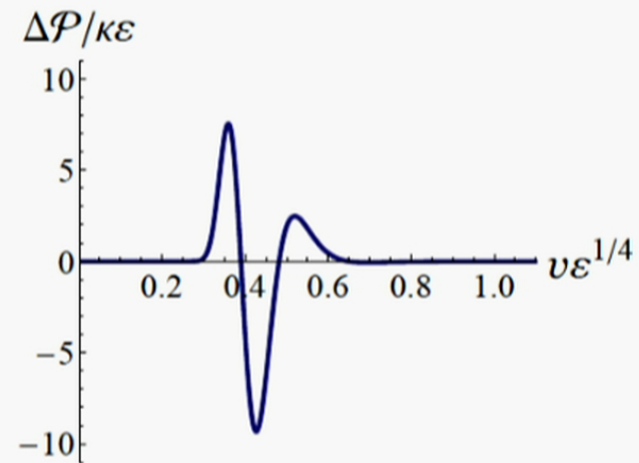
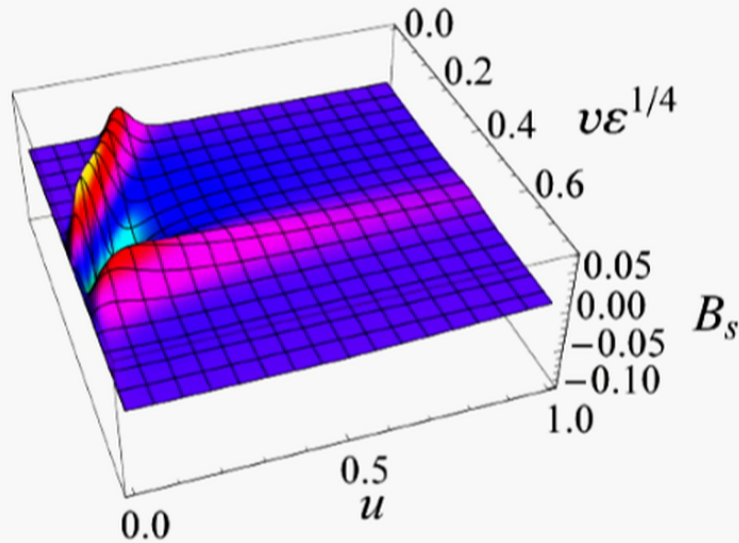


Results: Charged Plasma

Generic Evolution

$$B(v_0, r) = \mathcal{A} e^{-\frac{1}{2}(r-r_0)^2/\sigma^2}$$

$$\Delta\mathcal{P} \equiv \frac{1}{2}(T^{11} + T^{22}) - T^{33}$$

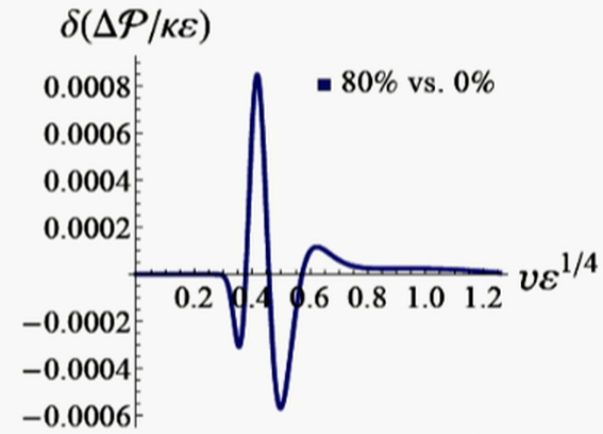
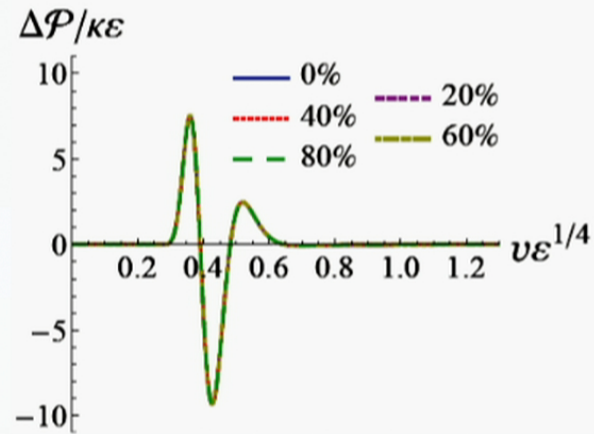


Results: Charged Plasma

ε held fixed

Anisotropy

$$(\rho_{\max} L^3)^4 = \frac{4}{3} m^3$$



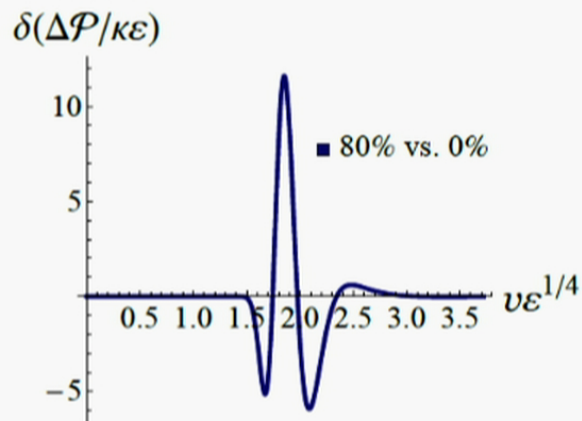
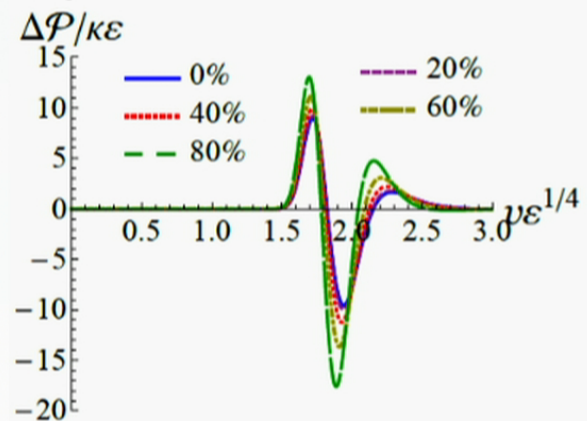
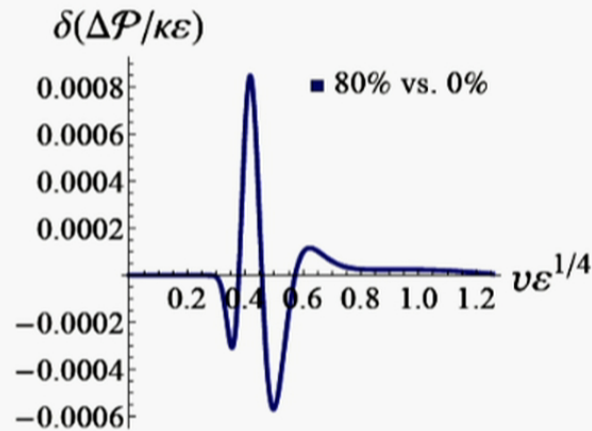
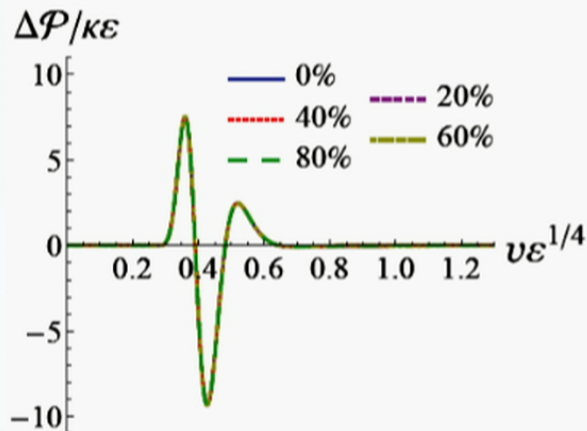
Results: Charged Plasma

ε held fixed

Anisotropy

$$(\rho_{\max} L^3)^4 = \frac{4}{3} m^3$$

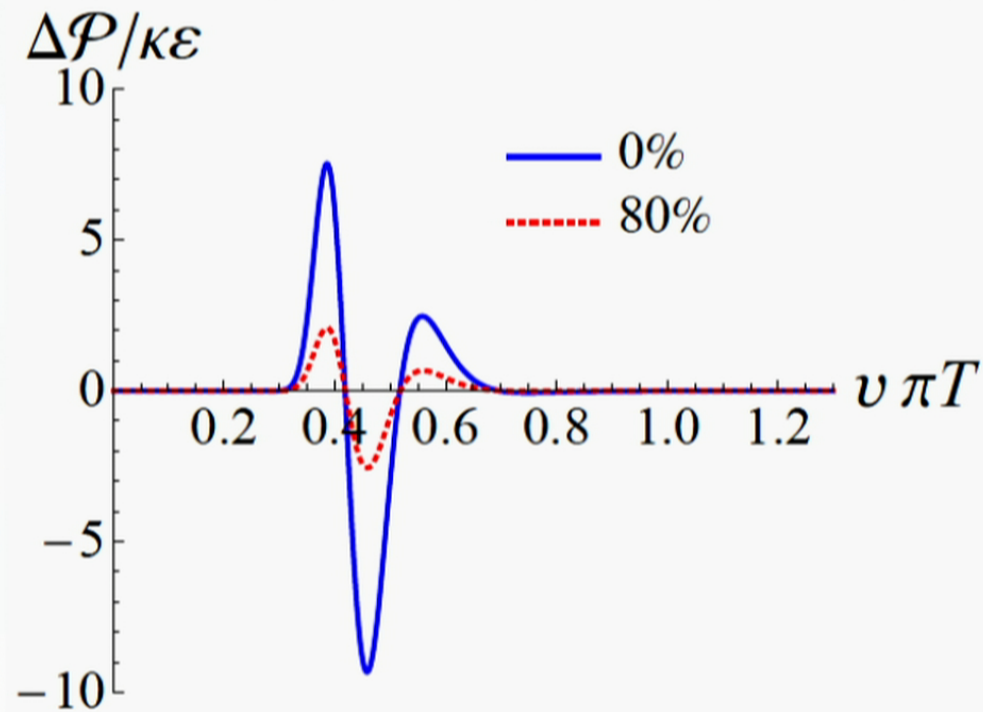
$$\mu/T = 0, 0.34, 0.73, 1.26, 2.21$$



Results: Charged Plasma

Constant Temperature

- if we instead keep T fixed (as opposed to ε), and express time in units of T



Results: Charged Plasma

Quasi-normal Modes

From asymptotically late time of $\Delta\mathcal{P}/\kappa\mathcal{E}$

$$\sim e^{\lambda_I t} \cos[\lambda_R t + \phi]$$

Charged ($\rho \neq 0, \mathcal{B} = 0$)

ρ/ρ_{\max}	$\text{Re } \lambda/\varepsilon^{1/4}$	$\text{Im } \lambda/\varepsilon^{1/4}$	Linearized $\lambda/\varepsilon^{1/4}$
0.0	3.35208 ± 0.00004	-2.95144 ± 0.00013	$3.35207 - 2.95150 i$
0.1	3.34564 ± 0.00016	-2.95468 ± 0.00019	$3.34568 - 2.95460 i$
0.2	3.32624 ± 0.00020	-2.96429 ± 0.00019	$3.32630 - 2.96444 i$
0.3	3.29319 ± 0.00028	-2.98266 ± 0.00036	$3.29327 - 2.98287 i$
0.4	3.24572 ± 0.00007	-3.01376 ± 0.00008	$3.24574 - 3.01377 i$
0.5	3.18366 ± 0.00016	-3.06498 ± 0.00007	$3.18370 - 3.06491 i$
0.6	3.11311 ± 0.00002	-3.15177 ± 0.00002	$3.11311 - 3.15176 i$
0.7	3.07021 ± 0.00006	-3.29402 ± 0.00006	$3.07022 - 3.29399 i$
0.8	3.11863 ± 0.00265	-3.41376 ± 0.00295	$3.11848 - 3.42004 i$

Charged Plasma Summary

- charge sensitivity more pronounced with pulses originating **closer to horizon**
- non-linearity sizes comparable to what was seen for neutral plasma
- **low sensitivity to charge density** when ε held fixed
- **low sensitivity to charge density** when T held fixed

Black Brane

$$(dx^i)^2$$

$$\frac{L^4}{\tilde{r}^4}$$

$$(L^2/\tilde{r}_h)^2$$

$$\frac{0^4}{8}$$

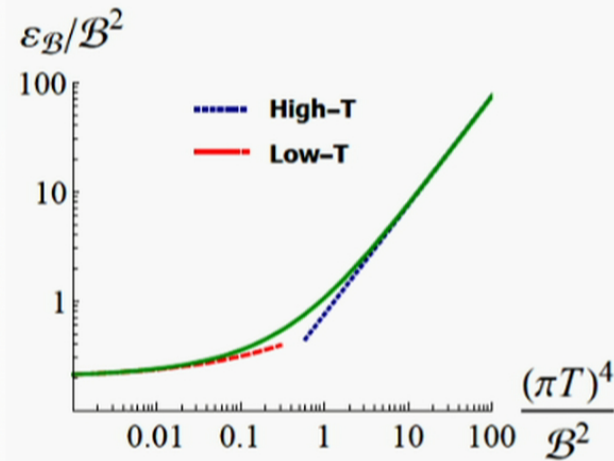
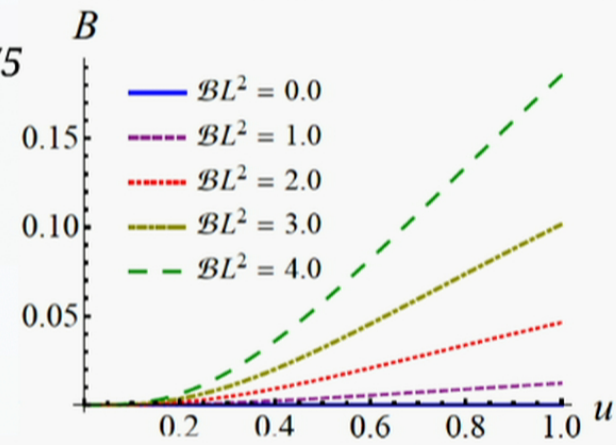
Magnetized Plasma

$$(\rho = 0, \mathcal{B} \neq 0)$$

Equilibrates to Magnetic Black Brane (Numerical Solution)

D'Hoker, Kraus 0908.3875

Anisotropy in the EQ case.
 \mathcal{B} picks a direction.

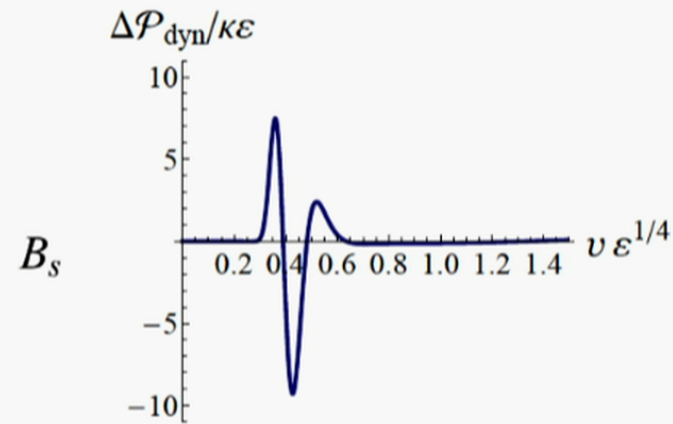
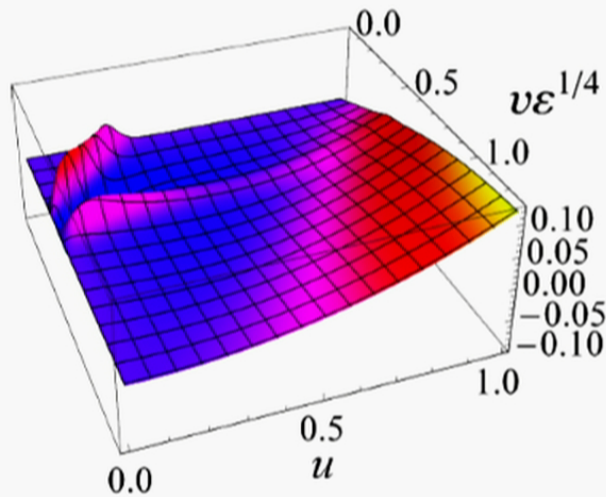


Results: Magnetized Plasma

Generic Evolution

$$B(v_0, r) = \mathcal{A} e^{-\frac{1}{2}(r-r_0)^2/\sigma^2} + \frac{1}{3}\mathcal{B}^2 r^{-4} \ln r$$

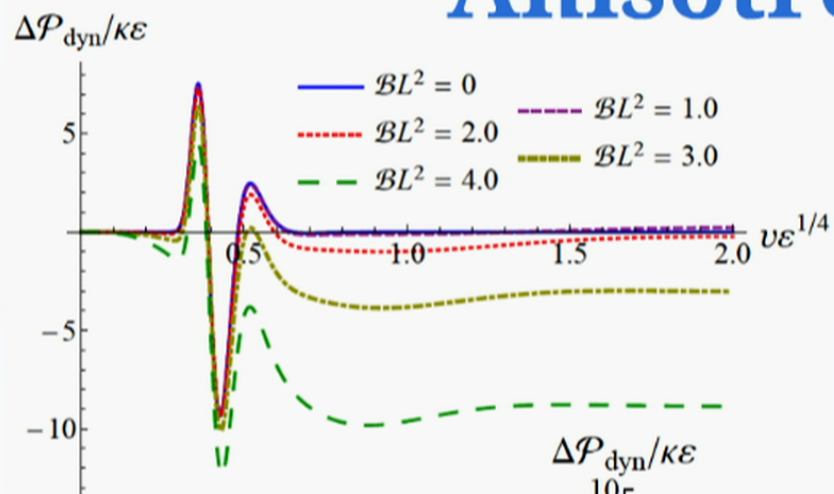
$$\Delta\mathcal{P}_{\text{dyn}} \equiv \frac{1}{2}(T^{11} + T^{22}) - T^{33} + \frac{1}{4}\kappa\mathcal{B}^2$$



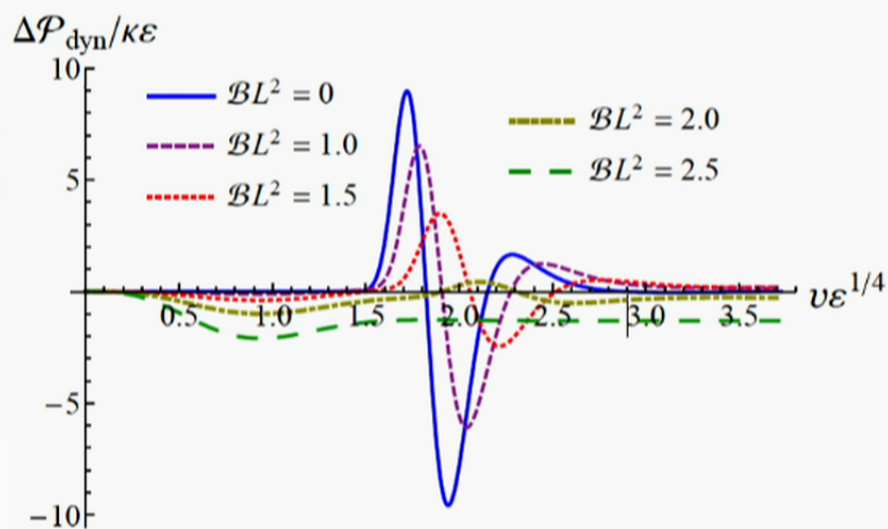
Results: Magnetized Plasma

Anisotropy

ε_L held fixed



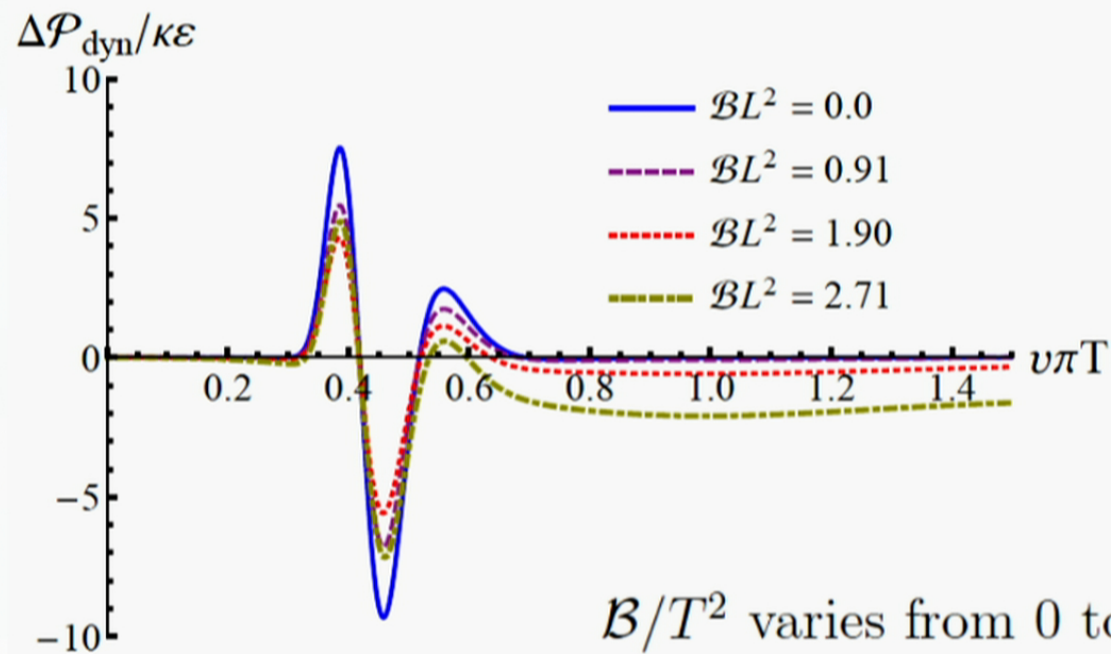
$\mathcal{B}/T^2 = 0, 13.0, 30.2, 30.5, 26.3$



Results: Magnetized Plasma

Constant Temperature

- if we instead keep T fixed (as opposed to ε_L), and express time in units of T



Results: Magnetized Plasma

Quasi-normal Modes

From asymptotically late time of $\Delta\mathcal{P}_{\text{dyn}}/\kappa\mathcal{E}$

$$\sim e^{\lambda_I t} \cos[\lambda_R t + \phi]$$

Magnetic ($\mathcal{B} \neq 0, \rho = 0$)

\mathcal{B}/T^2	$\varepsilon_{\mathcal{B}}/T^4$	$\bar{\mathcal{P}}/\kappa T^4$	$\Delta\mathcal{P}/\kappa T^4$	$\text{Re } \lambda/\varepsilon_{\mathcal{B}}^{1/4}$	$\text{Im } \lambda/\varepsilon_{\mathcal{B}}^{1/4}$	$\lambda/(\pi T)$
0	73.06	24.35	0	3.3521 ± 0.0001	-2.9514 ± 0.0001	$3.1195 - 2.7466 i$
0.990	72.98	24.16	-1.13	3.357 ± 0.001	-2.93 ± 0.06	$3.124 - 2.73 i$
5.344	80.74	22.15	-10.60	3.372 ± 0.002	-2.92 ± 0.06	$3.217 - 2.79 i$
12.953	125.85	13.98	-15.76	3.264 ± 0.007	-2.78 ± 0.01	$3.480 - 2.96 i$
17.821	170.16	3.79	-9.36	3.161 ± 0.002	-2.69 ± 0.04	$3.634 - 3.09 i$
22.836	226.69	-11.35	5.00	3.061 ± 0.008	-2.60 ± 0.03	$3.780 - 3.21 i$
30.161	328.21	-42.21	39.97	2.94 ± 0.01	-2.49 ± 0.03	$3.98 - 3.38 i$

Results: Charged Plasma

Charged Plasma Summary

- charge sensitivity more pronounced with pulses originating **closer to horizon**
- non-linearity sizes comparable to what was seen for neutral plasma
- **low sensitivity to charge density** when ε held fixed
- **low sensitivity to charge density** when T held fixed

Results: Magnetized Plasma

Magnetized Plasma Summary

- magnetic sensitivity more pronounced with pulses originating **closer to horizon**
- non-linearity sizes comparable to what was seen for neutral plasma
- **low sensitivity to magnetic field** when ε_L held fixed
- **low sensitivity to magnetic field** when T held fixed

Discussion

Conclusions

What have we we learned?

Discussion

Conclusions

What have we we learned?

To a good (often extremely good) level of accuracy:

- the pressure anisotropy is a **linear functional** of the initial anisotropy profile
- the timecourse is **insensitive** to **charge density** or **magnetic field** when the initial pulse profile is held fixed and either:

Discussion

Simple Model

Consider the time of peak anisotropy in the charged case, t_{peak} , as a function of equilibrium parameters and initial profile parameters

$$t_{\text{peak}}/L = f(\varepsilon L^4, TL, r_0/L, \sigma/L, \mathcal{A})$$

where we've exchanged charge fraction, ρ/ρ_{max} , for T

- small non-linearity size: indep of \mathcal{A}
- consider small width pulses, or for non-negligible width combine r_0 and σ

$$t_{\text{peak}}/L \approx g(\varepsilon L^4, TL, r_{\text{eff}}/L) \quad r_{\text{eff}} = r_0 + n\sigma$$

$$t_{\text{peak}}/L \approx g(\varepsilon L^4, TL, r_{\text{eff}}/L) \quad r_{\text{eff}} = r_0 + n\sigma$$

- our results show small dependence on charge density **at fixed energy density** - i.e. **indep of temp**
- also results show small dependence on charge density **at fixed temp** - i.e. **indep of energy density**

Main dependence on **effective depth of initial pulse**

$$t_{\text{peak}}/L \approx h(r_{\text{eff}}/L)$$

functional form limited by scaling relations, we find:

Discussion

Scaling Relations

$$x \rightarrow \tilde{x} = \alpha^{-1} x \qquad r \rightarrow \tilde{r} = \alpha \gamma^{-2} r$$

$$\tilde{B}(\tilde{x}, \tilde{r}) \equiv B(x(\tilde{x}), r(\tilde{r})),$$

$$\tilde{\Sigma}(\tilde{x}, \tilde{r}) \equiv (\alpha/\gamma) \Sigma(x(\tilde{x}), r(\tilde{r})),$$

$$\tilde{A}(\tilde{x}, \tilde{r}) \equiv (\alpha/\gamma)^2 A(x(\tilde{x}), r(\tilde{r})),$$

$$\tilde{L} \equiv \gamma^{-1} L \qquad \tilde{\mathcal{B}} \equiv \alpha^2 \mathcal{B} \qquad \tilde{\rho} \equiv \alpha^3 \rho$$

$$\alpha = \gamma$$

scaling by dimension

Discussion

Scaling Relations

$$x \rightarrow \tilde{x} = \alpha^{-1} x \qquad r \rightarrow \tilde{r} = \alpha \gamma^{-2} r$$

$$\tilde{B}(\tilde{x}, \tilde{r}) \equiv B(x(\tilde{x}), r(\tilde{r})),$$

$$\tilde{\Sigma}(\tilde{x}, \tilde{r}) \equiv (\alpha/\gamma) \Sigma(x(\tilde{x}), r(\tilde{r})),$$

$$\tilde{A}(\tilde{x}, \tilde{r}) \equiv (\alpha/\gamma)^2 A(x(\tilde{x}), r(\tilde{r})),$$

$$\tilde{L} \equiv \gamma^{-1} L \qquad \tilde{\mathcal{B}} \equiv \alpha^2 \mathcal{B} \qquad \tilde{\rho} \equiv \alpha^3 \rho$$

$$\alpha = \gamma$$

scaling by dimension

$$\alpha = 1, \gamma > 0$$

AdS radius scaling

$$t_{\text{peak}}/L \approx g(\varepsilon L^4, TL, r_{\text{eff}}/L) \quad r_{\text{eff}} = r_0 + n\sigma$$

- our results show small dependence on charge density **at fixed energy density** - i.e. **indep of temp**
- also results show small dependence on charge density **at fixed temp** - i.e. **indep of energy density**

Main dependence on **effective depth of initial pulse**

$$t_{\text{peak}}/L \approx h(r_{\text{eff}}/L)$$

functional form limited by scaling relations, we find:

$$t_{\text{peak}} \approx CL^2/r_{\text{eff}}$$

Discussion

Simple Model

Same argument goes for our Magnetic results,
with the replacements

$$t_{\text{peak}}/L = f(\varepsilon_L L^4, \mathcal{B}L^2, r_0/L, \sigma/L, \mathcal{A})$$

$$t_{\text{peak}}/L \approx g(\varepsilon_L L^4, \mathcal{B}L^2, r_{\text{eff}}/L)$$

$$t_{\text{peak}} \approx CL^2/r_{\text{eff}}$$

For charged *and* magnetized plasmas our model suggests:

$$t_{\text{peak}} \approx CL^2/r_{\text{eff}}$$

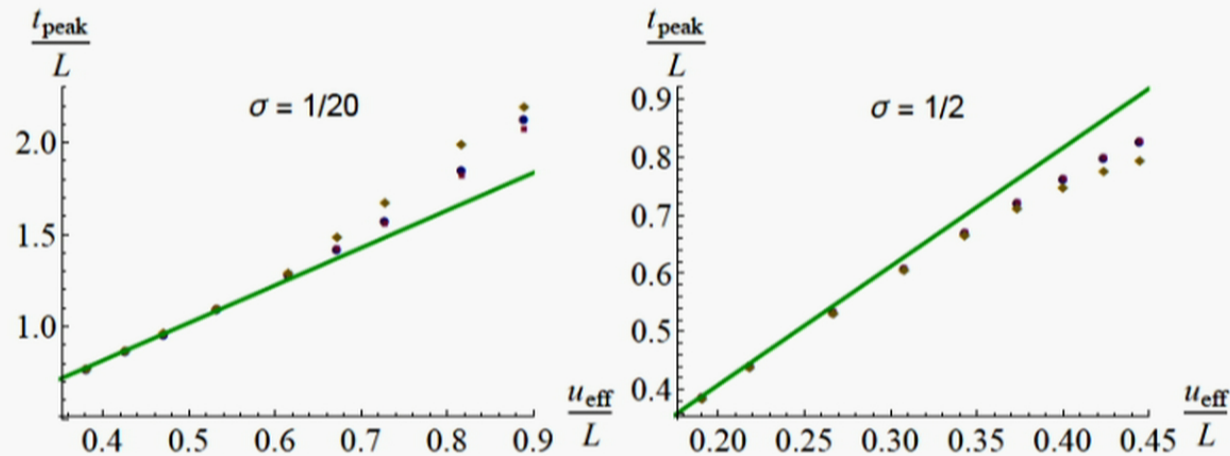
Discussion

Comparison to Model

We test against a sharper width pulse, and wider pulse, in uncharged, charged, and magnetized plasmas, at varying depths.

$$t_{\text{peak}} \approx CL^2/r_{\text{eff}} \quad r_{\text{eff}} = r_0 + n\sigma$$

We find good agreement using $n = 2.5$, and $C \approx 2.04$



Conclusions

- developed far-from-equilibrium numerical evolution to include **charge density** and **magnetic fields** (including log difficulties).
- explored the **surprising amount of linearity** exhibited by the evolution.
- found that both a **substantially large** chemical potential or magnetic field has a **very small effect on equilibration times** - and developed **a simple model**.
- We see that **changing the balance between fermions and scalars** (via chemical potential) **has negligible effect**, suggesting insensitivity to the precise makeup of the plasma -- small confidence boost in the applicability of $N=4$ as a proxy for QCD.